Contents lists available at ScienceDirect

Combustion and Flame

Effect of iron and boron ultrafine powders on combustion of aluminized solid propellants

Alexander G. Korotkikh [a,b,*], Oleg G. Glotov [c], Vladimir A. Arkhipov [b], Vladimir E. Zarko [c], Alexander B. Kiskin [c]

[a] *Institute of Power Engineering, Tomsk Polytechnic University, 30, Lenin Ave, Tomsk 634050, Russia*
[b] *Research Institute of Applied Mathematics and Mechanics, Tomsk State University, 36, Lenin Ave., Tomsk 634050, Russia*
[c] *Institute of Chemical Kinetics and Combustion, Siberian Branch of the Russian Academy of Sciences, 3, Institutskaya Str., Novosibirsk 630090, Russia*

ARTICLE INFO

ABSTRACT

The paper presents the results of measurement of the burning rate of aluminized composite solid propellants (CSPs) and parameters of sampled condensed combustion products including their particle size distribution, chemical and phase composition. Effect of ultra-fine iron and amorphous boron additives in CSP formulations based on AP, butadiene rubber and Alex (2 wt. %) on the combustion characteristics was studied. The sampled particles of condensed combustion products (CCPs) were classified as oxide particles (less than 55 μm) and agglomerate particles (up to 500 μm). The CCPs particles were subjected to morphological, particle size, chemical and phase analyses. It was found that partial replacement of Alex by 2 wt. % of iron in CSP leads to 1.3-1.4 fold increase in the burning rate in the pressure range of 2.2-7.5 MPa. At the same time the agglomeration of metal fuel is slightly increased: the mean diameter of agglomerate particles in CCPs is increased up to 1.2 fold and their content is increased up to 1.4 fold. The content and mean diameter of oxide particles in CCPs are reduced by 16 % and 13 %, respectively. Upon partial replacement of Alex by 2 wt. % of boron the burning rate is practically unchanged as compared with that for basic propellant with Alex. However the agglomeration is significantly enhanced, which is manifested at the increase in the agglomerate particles content in CCPs by 1.8-2.2 times, increase by 1.6-1.7 times in the agglomerates mean diameter and increase in the unburned metal fraction in agglomerates by 1.6-1.9 times. The content and the mean diameter of the oxide particles are reduced more significantly than in the case of iron introduction, namely, by 20-30 % and 30-40 %, respectively.

© 2017 The Combustion Institute. Published by Elsevier Inc. All rights reserved.

1. Introduction

The modern composite solid propellants (CSPs) contain as an oxidizer the crystals of ammonium perchlorate (AP), ammonium nitrate (AN) and nitramines (cyclotrimethylenetrinitramine RDX, cyclotetramethylenetetranitramine HMX or hexanitrohexaazaisowurtzitane HNIW (CL-20) [1–7]), a binder, which can be inert or energetic polymer [8–10], and a metal fuel (mainly aluminum) in the form of powder of various dispersity with typical content up to 22 wt.% [11]. As the combustion catalysts for CSPs there are used copper, iron, zinc, cadmium, metal oxides (MnO_2, Ni_2O_3, Cr_2O_3, MgO, Fe_2O_3, Co_2O_3, Co_3O_4, SiO_2), and magnesium salts of chromic and metachromic acids, complex cyanides of cop-

per, iron and nickel, organometallic compounds [12–16]. The most common and universal catalysts are the systems containing copper, chromium and iron atoms [17–19].

Control of the CSP burning rate is mainly achieved by introducing in solid propellant formulation the catalysts, as well as by partial or complete replacement of AP and AN by nitramines that changes the equivalence ratio of formulation, or by varying the particle size of oxidizer and metal powders [20–23]. Promising metallic fuels are highly dispersed aluminum powders, which are characterized by different dispersity and passivation method, as well as bimetallic powders or mixtures of aluminum and other metals, their alloys, and metal powders with various coatings [24–31]. Previously, it was found that ultra-fine powders (UFPs) of metals, produced by technology of conductors electrical explosion [32], are highly reactive in oxidation reactions and have a number of properties that differ them from micron powders: the presence of oxide-hydroxide layer and hydrogen on the surface of particles and an existence of aggregated particles formed in the processes

---

* Corresponding author at: Institute of Power Engineering, Tomsk Polytechnic University, 30, Lenin Ave, Tomsk 634050, Russia.

E-mail address: korotkikh@tpu.ru (A.G. Korotkikh).

of manufacturing or passivating and storage of powders; the existence of internal pores in the structure of aggregated particles and the electrostatic field at the surface or subsurface layers of particles [33].

The main combustion characteristics of CSPs regarding the propulsion systems applications are the dependency of linear burning rate on pressure, the value of specific impulse [20] equal to the increase in thrust value realized at the firing of unit mass of solid propellant, and chemical and granulometric composition of the combustion condensed products (CCPs). Different methods for modifying the metallic fuel can make effect on different characteristics of solid propellants combustion. The magnitude of the burning rate and the agglomeration parameters, including the combustion completeness of metal fuel, at present practically cannot be estimated correctly prior to experiment. Therefore, the effect of additives and other modifications of propellant formulations have to be examined mainly experimentally. The goal of this paper was studying the features of the combustion mechanism of metallized CSPs containing aluminum UFP (Alex) partially replaced by Fe or B UFP.

The paper describes the method of sampling the CCPs particles in a blow-through bomb to determine their particle size distribution, chemical and phase composition. The experimental results on agglomeration and combustion characteristics of CSPs based on ammonium perchlorate, butadiene rubber and ultra-fine aluminum (Alex type), containing additives of iron and boron, are presented.

2. Experimental

2.1. The tested CSP samples

The investigations were performed with basic CSP formulation (# 1) containing two fractions of AP (sieve fractions less than 50 µm and 160–315 µm with mass ratio 40/60), butadiene rubber plasticized by transformer oil (19.7 wt.%), and aluminum UFP Alex (15.7 wt.%) obtained in argon using the technology of electric explosion of conductor. In formulations # 2 and # 3 Alex was partially replaced by 2 wt.% catalyst additive – UFPs of iron or amorphous boron. According to the measurements performed with the BET surface area analyzer Nova 2200e in nitrogen, the specific surface area comprised $7.04 \, m2/g$ for Alex, $1.08 \, m2/g$ for iron, and $8.63 \, m2/g$ for amorphous boron. Micrographs of scanning electron microscope Jeol JSM-7500F of particles of Alex, iron and amorphous boron are shown in Fig. 1. According to the manufacturers data the original substance content in tested Alex comprised 85 wt.%, iron UFP – 92 wt.%, and boron UFP – 99.5 wt.%

Note that the particles of metal UFPs obtained by the technology of electric conductors explosion in different gaseous environments during storage are usually aggregated and adsorb up to 7 wt.% of gases (for aluminum mostly hydrogen) [33]. The final formation of composite propellants structure is possibly accompanied by changing the size distribution of aggregated metal particles in the course of mixing process [22].

The tested cylindrical samples of CSPs of 10 mm diameter and of 30 mm height were manufactured in laboratory conditions by means of mixing the components followed by extrusion of mixture and its solidification in a drying oven. The density of tested CSP samples depending on the components composition was in the range of $1.53–1.59 \, g/cm^3$.

2.2. Combustion of CSPs

The study of the effect of ultra-fine iron and amorphous boron additives on the burning rate of CSPs and CCPs characteristics was carried out using a blow-through sampling bomb. The basic installation option has been presented in [34]. Extinguishing the parti-
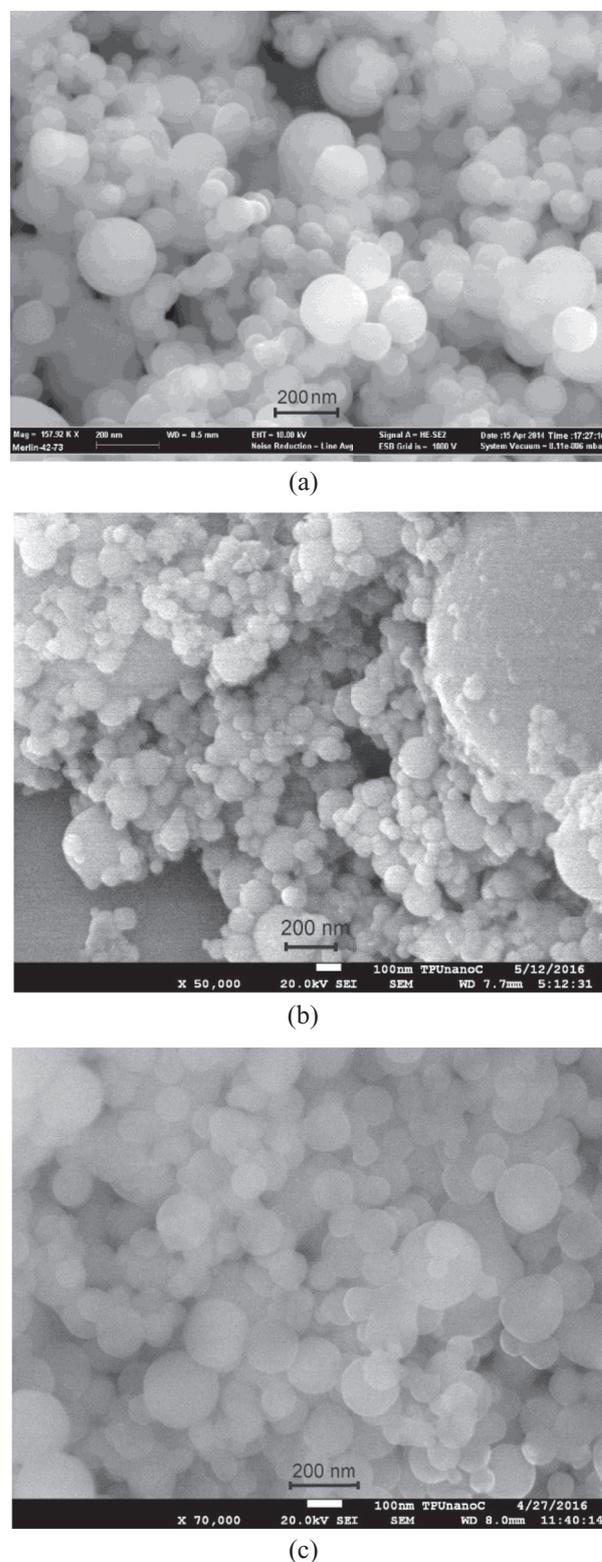

(a)

(b)

(c)

Fig. 1. SEM images of virgin aluminum Alex (a), iron (b) and boron (c) UFPs.

cles leaving the burning surface of tested sample of solid propellant occurred due to mixing the combustion products of CSP with a co-current flow of inert gas. A stack of metal sieve screens and an analytical aerosol filter type AFA were used for trapping the particles. The advantages of method are the possibilities of operation under elevated pressures (up to 15 MPa), the wide variation of particles quenching location (20–200 mm from the burning surface),
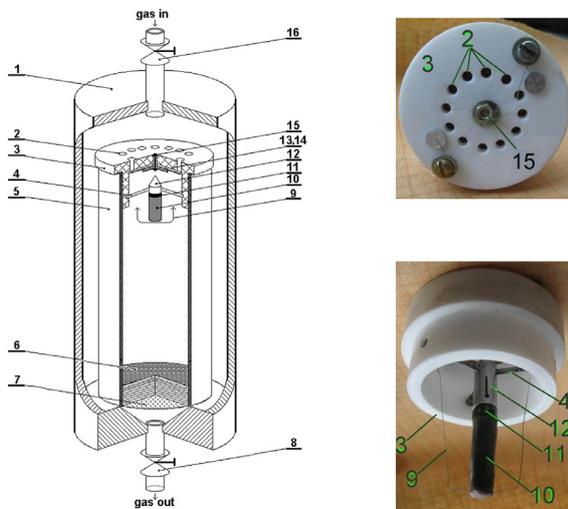
Fig. 2. The scheme of the blow-through sampling bomb: 1 – body of bomb; 2 – holes; 3 – top cover of inner cylinder; 4 – needles; 5 – thin-walled inner cylinder; 6 – stack of metal sieve screens; 7 – aerosol filter; 8 – outlet valve; 9 – igniting wire; 10 – sample of CSP; 11 – pedestal; 12 – cowl; 13 – rubber disk; 14 – Teflon disk; 15 – central screw; 16 – inlet valve.

and a wide range of sampled particles sizes (from nanometers to centimeters). It allows studying the fine oxide and the coarse agglomerate particles characteristics. In the present work we used an improved version of the installation containing valve blocking the release of particles into a free volume of bomb. The lateral surface of samples was coated with inhibiting layer made of heat-resistant rubber Solprene® (a styrene/butadiene copolymer). During combustion of heat-resistant rubber the carbonaceous particles were formed, but their content in CCPs did not exceed 1 wt.%. Plexiglas pedestal was glued to the rear end of CSP sample. A thin layer of the metal-free igniting paste was attached at the front end of CSP sample. The use of relatively small diameter samples (10 mm) and combustible heat-resistant coating rubber allowed carrying out quenching the CCPs particles close to the sample burning surface (at a distance of ∼ 30 mm).

The scheme of the blow-through sampling bomb is presented in Fig. 2. The CSP sample (10) was placed on a pedestal (11) with cowl (12) and attached to the top cover (3) by means of three needles (4). Then this assembly was inserted into a thin-walled inner cylinder (5), which was placed inside the blow-through bomb body (1). During experiment, the bomb was continuously blown by nitrogen, which moved from a high pressure container through an inlet valve (16). A top cover (3) is provided with a valve, which consists of a rubber disk (13) and Teflon disk (14) pressed to cover by means a central screw (15). In the initial position a rubber disc (13) closes the holes (2) of top cover (3). When bomb is blown by nitrogen the limb of rubber disk (13) turns up that releases gas into a cylinder (5). When igniting a CSP sample (10) by a nichrome wire (9), the pressure of gas in an inner cylinder (5) was increased, and a valve of cover was locked by means of pressing a rubber disk (13) to holes (2) of cover (3) like it was done in the initial position.

The pressure of gas in the blow-through bomb was controlled by the manometer and the pressure sensor LKh-412 type. The required pressure and gas flow values were adjusted by means of inlet (16) and outlet (8) valves. The gas flow rate was controlled at the outlet of the bomb using the float-type flowmeter (rotameter) and the Venturi tube equipped with U-tube manometer.

Experiments were carried out in nitrogen at three pressure levels p: 2.2, 4.5 and 7.5 MPa. The burning rate of CSPs was determined on the basis of known initial length and the burning time of sample which was measured via processing the signal from a pres-

sure sensor installed in a bomb. The sampled particles of combustion products were first divided into 4 fractions: less than 80 μm, 80–160 μm, 160–315 μm and larger than 315 μm. Then the CCPs particles were subjected to morphological, particle size, chemical and phase analyses.

2.3. The properties of CCPs

Particle size analysis of CCPs was performed with the use of the Malvern 3600E laser particle sizer for fractions less than 80 μm, and with the use of an optical microscope for coarse CCPs fractions. Chemical analysis of CCPs particles was performed by permanganatometric method [35] which determined the amount of active (unburned) aluminum.

The results of the particle size and chemical analyses were presented in the form of histograms of the size distribution density of the relative mass of CCPs particles:

- $f_i(D) = m_i/(M_{prop} \cdot D_i)$,

and of the relative mass of unburned aluminum in CCPs particles

- $f_i^{Al}(D) = f_i(D) \cdot \varepsilon_j^{Al}$,

where m_i is the mass of CCPs in the ith histogram interval, M_{prop} is the mass of solid propellant (total for all samples burned in series at given conditions), D_i is the width of the ith histogram interval, ε_j^{Al} is the weight content of unburned aluminum in the jth sieve fraction, which includes ith histogram interval. Later the index i is omitted and the functions are briefly called «mass distribution».

Usually the functions $f(D)$ and $f^{Al}(D)$ have a pronounced local minimum D_L [36]. The particles with sizes at the left from the minimum (with $D < D_L$) are substantially free of unreacted aluminum and usually are called as fine or oxide particles. Unburned aluminum is concentrated in larger size particles with diameter $D > D_L$, which have the agglomerate origin and, therefore, are called agglomerates. The fine oxide particles and coarse agglomerate particles were examined separately. Analyzing the functions $f(D)$ and $f^{Al}(D)$ we calculated a set of dimensionless mass parameters (parameter value divided by the weight of CSP). For example, $m_f = M_f/M_{prop}$ is dimensionless weight of fine particles, where M_f and M_{prop} are the weights of fine particles of CCPs and solid propellant. Using function $f(D)$, we calculated the mean diameters D_{mn} of oxide and agglomerate particles in the ranges ($D_{min} < D < D_L$) and ($D_L < D < D_R$), respectively. Below we will deal with the following moment-based mean diameters D_{mn}: for agglomerate particles D_{43}^{ag} and for oxide particles D_{30}^{ox}.

The agglomerate particles size are characterized by D_{43}^{ag} mean diameter, which is also called as volume mean diameter. Note that some physical methods (light scattering diffraction, sedimentation, sieving) give D_{43} without measuring parameters of individual particles. The oxide particles are characterized by D_{30}^{ox} mean diameter (also called as mean volume diameter). Similarly, there are physical methods and device (Coulter counter) which measure directly D_{30}. However, in this case the separate particles should be measured and counted. The D_{30} mean diameter is used to characterize fine particles because it represents the main tendencies of their size distribution function and herewith it is less scattering than D_{32} and D_{43} calculated in the size range $D_{min} < D < D_L$. To calculate the D_{mn}, with use of Eq. (1), see below, the mass histogram is recalculated into the number (frequency) histogram taking into account experimentally measured values of the particle density.

Values of D_L and D_R were determined using the $f(D)$ function. In this paper $D_{min} = 0.5$ μm is the minimum size of particles detected by Malvern 3600E and $D_L = 55$ μm is the boundary between the fine particles and agglomerates (corresponding to the right boundary of the 15th size interval of Malvern's histogram). D_R is

Table 1
Results of thermodynamic calculations.

Propellant No., metal fuel	Parameters							
	I, kJ/kg	T_{ad}, K	k	μ, g/mol	α	J, m/s	z_c, z_a	Condensed products composition
1, Alex	−2228	2561	1.19	17.0	0.422	2519	0.263	$[Al_2O_3]_c$ – 100%
							0.276	$[Al_2O_3]_a$ – 100%
2, Alex+Fe	−2179	2477	1.20	17.5	0.424	2455	0.237	$[Al_2O_3]_c$ – 100%
							0.241	$[Al_2O_3]_a$ – 100%
3, Alex+B	−2179	2366	1.20	18.0	0.409	2517	0.200	$[Al_2O_3]_c$ – 100%
							0.293	$[Al_2O_3]_a$ – 82%
								$[B_2O_3]_a$ – 9%
								$[BN]_a$ – 9%

Index «c» stands for the combustion chamber and «a» for the nozzle exit section, $p_c/p_a = 4.0/0.1$ (MPa).

the maximum size of agglomerates ($D_R = 310 \,\mu m$ for the formulation with Alex; $D_R = 480 \,\mu m$ for the formulation with Alex+B, and $D_R = 610 \,\mu m$ for the formulation with Alex+Fe).

The general formula for calculating the moment-based mean diameters of particles is

$$D_{mn} = \sqrt[m-n]{\left(\sum_{i=1}^{k} D_i^m \cdot N_i\right) \Big/ \left(\sum_{i=1}^{k} D_i^n \cdot N_i\right)}, \tag{1}$$

where m, n are integer numbers defining the order of the mean size, k is the number of dimensional intervals in cumulative histogram, N_i is the number of particles in the ith interval, D_i is the middle of ith interval.

In this work we used the following parameters:

m_f is the mass of fine oxide particles,

m^{Al}_f the mass of unburned aluminum in oxide particles,

m_{ag} the mass of agglomerate particles,

m^{Al}_{ag} the mass of unburned aluminum in agglomerates,

$m_{ccp} = m_f + m_{ag}$ the total mass of CCPs,

$m^{Al}_{ccp} = m^{Al}_f + m^{Al}_{ag}$ the total mass of unburned aluminum in CCPs,

$m^{Al}_{prop} = 0.157$ the initial mass of aluminum in propellant,

$\eta = m^{Al}_{ccp}/m^{Al}_{prop}$ incompleteness of aluminum combustion,

$Z_m^a = [m^{Al}_{ag} + (9/17) \cdot m_{ag} - m^{Al}_{ag}]/m^{Al}_{prop}$ the fraction of metal involved in the agglomerates formation [37],

$\Pi = m_{ccp}/\{m_{ccp} + [m^{Al}_{prop} - m^{Al}_{ccp} \cdot (8/17) - m_{ccp} \cdot (9/17)]/(m^{Al}_f/m_f + 9/17)\}$ is the representativeness of sampling equaled to the ratio of actually sampled and theoretically calculated mass of CSPs.

The last formula was obtained from the mass balance relationships using the following assumptions: (1) aluminum powder in CSPs contains 100 wt.% of active aluminum; (2) CCPs of propellant contain only aluminum and aluminum oxide Al_2O_3; (3) procedure for the sampling and preparation of CCPs provides a complete sampling the coarse agglomerate particles and the CCPs mass deficit can only be due to the loss of fine particles.

It should be noted that the values of parameters presented in Table 2, which were calculated with the use of chemical analysis data, are approximate because it was taken $m^{Al}_{prop} = 0.157$. In the first approximation we considered that the metal fuel in all formulations consists of 100 wt.% aluminum, and also we assumed that the presence of boron and iron does not make sizable effect on the results of aluminum determination in permanganatometric analysis. At the same time it is known that the content of active aluminum in UFPs can be significantly lower (for example, for Alex ∼ 85–88 wt.% [33,35]). For obtaining more accurate results, when using the combined metal fuel, special methods for chemical analysis should be used (or be developed). Thus, for a metal fuel based on aluminum and boron a cerimetric method can be used [38].
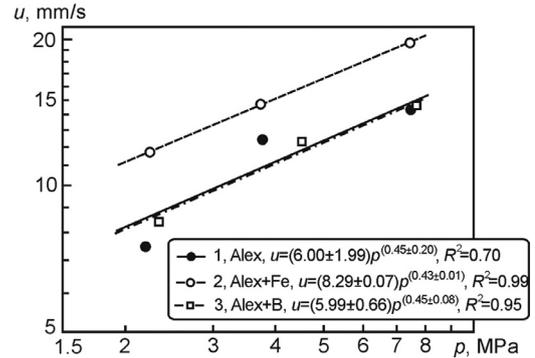

Fig. 3. The burning rate of propellants vs pressure.

3. Results and discussion

3.1. Combustion characteristics of CSPs

3.1.1. Thermodynamic calculations

Usually a modification of metal fuel reduces theoretical value of CSP specific impulse. Along with that some peculiar effects may appear which are illustrated in this paragraph. For theoretical estimation of the effect of iron and boron additives on the energetic characteristics of aluminized CSPs and on the composition of CCPs the thermodynamic calculations were carried out of the equilibrium composition of the combustion products for tested propellants, using the code «TERRA» [39]. Table 1 shows the calculated values of the enthalpy I of propellants, the adiabatic combustion temperature T_{ad}, the equilibrium adiabatic index k, the molecular mass of gaseous combustion products μ at pressure in the combustion chamber $p_c = 4.0$ MPa, and the ox-red elements ratio α which is calculated for the propellant formulation as a whole. For the value of gas flow expansion $p_c/p_a = 4.0/0.1$ MPa (the pressure at the nozzle exit section $p_a = 0.1$ MPa) there are presented the values of specific impulse J, and the mass fraction of condensed phase products within the combustion chamber z_c and at the nozzle exit section z_a. In the calculations, we assumed that Alex UFP is a mixture of Al and Al_2O_3 in the mass percentage of 85/15.

3.1.2. Experimental data

Figure 3 shows the dependencies of the burning rate on pressure for tested propellants in the form

$$u = B \cdot p^n$$

where u in mm/s, p in MPa, and also the values of determination coefficient R^2 characterizing the quality of approximation.

As one can see the dependencies of burning rate on pressure for the propellants with Alex and Alex+B are matched up within

Table 2
Pressure, burning rate, mass and size parameters that characterize the condensed combustion products.

Propel-lant No., metal fuel	p, MPa	u, mm/s	%Al in the frac-tion <80 μm	%Al$_{av}$	η	m_{ccp}	m^{Al}_{ccp}	m_f	m^{Al}_f	m_{ag}	m^{Al}_{ag}	Π	D^{ox}_{30}, μm	D^{ag}_{43}, μm	$Z_m{}^a$
1, Alex	2.2	7.5	0.65 ± 0.03	1.64	0.0326	0.3116	0.0051	0.2639	0.0018	0.0477	0.0033	1.07	6.4	108	0.17
1, Alex	3.8	12.4	0.41 ± 0.01	1.21	0.0233	0.3017	0.0037	0.2400	0.0010	0.0582	0.0024	1.03	6.7	119	0.22
1, Alex	7.5	14.3	0.67 ± 0.09	0.98	0.0198	0.3168	0.0031	0.2567	0.0017	0.0601	0.0014	1.08	6.2	117	0.21
2, Alex+Fe	2.2	11.7	1.06 ± 0.01	1.7	0.0304	0.2747	0.0058	0.2208	0.0024	0.0540	0.0034	0.94	6.1	111	0.19
2, Alex+Fe	3.7	14.7	0.76 ± 0.03	1.1	0.0209	0.2894	0.0038	0.2283	0.0018	0.0609	0.0015	0.99	5.8	123	0.21
2, Alex+Fe	7.5	19.7	0.31 ± 0.01	1.54	0.0290	0.2963	0.0046	0.2176	0.0008	0.0788	0.0038	1.01	5.8	138	0.28
3, Alex+B	2.3	8.4	1.29 ± 0.05	2.62	0.0466	0.2791	0.0073	0.1854	0.0025	0.0937	0.0048	0.96	4.8	177	0.33
3, Alex+B	4.5	12.3	0.87 ± 0.03	1.81	0.0341	0.2949	0.0053	0.1928	0.0017	0.1020	0.0036	0.91	4.8	203	0.36
3, Alex+B	7.7	14.6	0.83 ± 0.01	1.56	0.0292	0.2930	0.0046	0.1881	0.0016	0.1050	0.0030	1.00	4.8	195	0.36

Notes:
(1) The calculated mass parameters are presented with four digits after the decimal point to avoid confusion due to rounding of small values. The confidence interval for these parameters is typically ∼ 10% at a confidence level 68% [7].
(2) The relative error of the oxide particles mean diameter D^{ox}_{30}, according to specifications of particle size analyzer Malvern 3600E, comprises 4%. The absolute error of determining the mean diameter of agglomerate particles D^{ag}_{43} amounts ∼ 9 μm.
(3) Propellant with Alex has $m_{ccp} > m_{ag} + m_f$ and $m^{Al}_{ccp} > m^{Al}_{ag} + m^{Al}_f$ in combustion process at $p = 3.8$ MPa. In this case, the CCPs have the abnormally large agglomerate particles, often non-spherical form. Such particles are probably formed by accumulation of metal on inhibiting layer. These were excluded from consideration at calculations of m_{ag}, m^{Al}_{ag}, D^{ag}_{43} by assigning of corresponding value D_R. However, aluminum containing in these large particles has been taken into account in calculation of m^{Al}_{ccp}, η and $Z_m{}^a$.

the range of experimental error. Partial replacement of 2 wt.% Alex by iron UFP practically does not change the exponent of burning rate law but leads to significant increase in the burning rate (from 7.5 to 11.7 mm/s at $p = 2.2$ MPa and from 14.3 to 19.7 mm/s at $p = 7.5$ MPa).

A noticeable increase in the burning rate of iron doped CSP can be possibly explained by the iron oxide catalytic effect on the oxidizer decomposition [40,41] and corresponding increase in the heat release on the burning surface of sample. Thermal analysis data obtained with TG/DSC analyzer Netzsch STA 449 F3 Jupiter at the heating rate of 10 K/min in argon have shown that the CSP beginning temperature of intensive decomposition is reduced by ∼ 20 K upon addition of iron UFP. Note that there is a possibility for thermite reaction between fine aluminum particles and iron oxide within subsurface reaction layer resulting in additional heat release [19] and in increase the surface temperature of CSP [42].

Additive of 2 wt.% boron in CSP formulation does not make catalytic effect on the propellant decomposition. The thermal analysis data show that the beginning temperature of intensive decomposition of CSP with Alex+B remains the same (582 K). Consequently, the burning rate of boron doped CSPs exhibits the same behavior as original Alex based CSP.

3.2. Characteristics of CCPs

Table 2 and Fig. 4 present the values of the mass and size parameters for sampled CCPs. Within the confidence intervals the scatter of the experimental data on the CCPs parameters (typical error bars in Fig. 4) is the same for all tested formulations.

3.2.1. Agglomerate particles

The relative mass of agglomerates m_{ag} (dark grey bars in Fig. 4) is increased with the growth of ambient pressure for all formulations of CSPs. In the case of propellants with Alex and Alex+Fe the values of parameters m_{ag}, $Z_m{}^a$, D^{ag}_{43} and η, characterizing the agglomerates properties are similar (Table 2).

At the partial replacement of Alex by boron the dimensionless mass of agglomerates m_{ag}, the fraction of agglomerates in CCPs m_{ag}/m_{ccp} and the fraction of metal involved in the formation of agglomerates $Z_m{}^a$ are increased. In addition, the agglomerates of propellant with Alex+B are much larger in size D^{ag}_{43}. Taking into account the similar levels of the burning rate, as well as the identity of the geometric structure of propellants (which is mainly determined by the coarse particles of AP), these facts should be defi-

nitely treated as an agglomeration intensification due to boron additive.

At the same time, despite the intensification of agglomeration in the presence of iron and especially of boron, all three propellants demonstrated relatively low incompleteness of metal combustion $\eta = 0.02$–0.03 (except $\eta \approx 0.05$ in the case of propellant with Alex+B at $p = 2.3$ MPa). It should be noted that for the tested CSP formulations the content of metallic aluminum in the fractions >80 μm (actually, in the agglomerates) in all cases has been in the range of 3–15%. This was significantly lower than the typical values of 20–60% for traditional propellants in the same combustion conditions. The unreacted aluminum content, %Al$_{av}$, averaged over all CCPs fractions was equal to 1–3% in all cases.

Values of sampling representativeness Π in the range of 0.91–1.08 correspond to typical level for used sampling technique.

Figure 5 shows the mass distribution of CCPs, i.e. the function $f(D)$ – size distribution density of CCPs particles relative mass. In such presentation the area under graph is proportional to the mass of CCPs. For all pressure levels, the distributions of agglomerate particles (with $D > D_L$, where $D_L = 55$ mm) in the case of propellant with Alex+B are more «massive» (histogram is wider and has a long right tail, the maximum is shifted to the right), which clearly indicates stronger agglomeration as compared to propellants with Alex and Alex+Fe.

Peculiar feature of the agglomerate particles size distributions for propellants with Alex and Alex+Fe is an existence of mode located at 100 μm, which provides a relatively large mass contribution in the range of 55–100 μm. The particles of given size range are the combustion residues of agglomerates. The following facts testify to the burning out of agglomerates. In the case of propellant with Alex with increase in pressure from 2.2 to 7.5 MPa the incompleteness combustion η is changed as the sequence $0.033 \rightarrow 0.023 \rightarrow 0.020$ (Table 2), and the content of metal aluminum in the particles of 80–315 μm sizes is decreased as ∼ 15% → 8% → 5% (data [43]). At the same time the mean diameter of agglomerate particles is slightly changed: 108 μm → 119 μm → 117 μm (the instrumental error ± 9 μm).

For propellant with Alex+B the burning out of agglomerates is manifested in redistribution of CCPs mass into interval of 55–100 μm. One can see that the mass content in this interval at pressure 7.7 MPa is noticeably larger than that at pressures of 2.3 and 4.5 MPa. At the increase in pressure from 2.3 to 7.7 MPa the incompleteness of combustion η is changed in the sequence of $0.047 \rightarrow 0.034 \rightarrow 0.029$; the content of metal aluminum in particles of 80–315 μm is decreased as ∼ 5% → 4% → 3% [43]). The mean
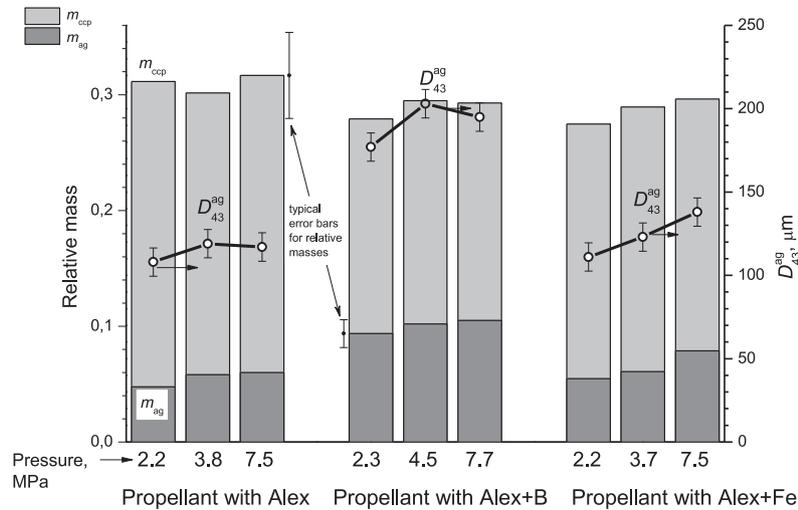
Fig. 4. Agglomerate mean diameter D_{43}^{ag}, dimensionless values of agglomerate mass m_{ag} and CCPs mass m_{ccp} for propellants at different pressures.
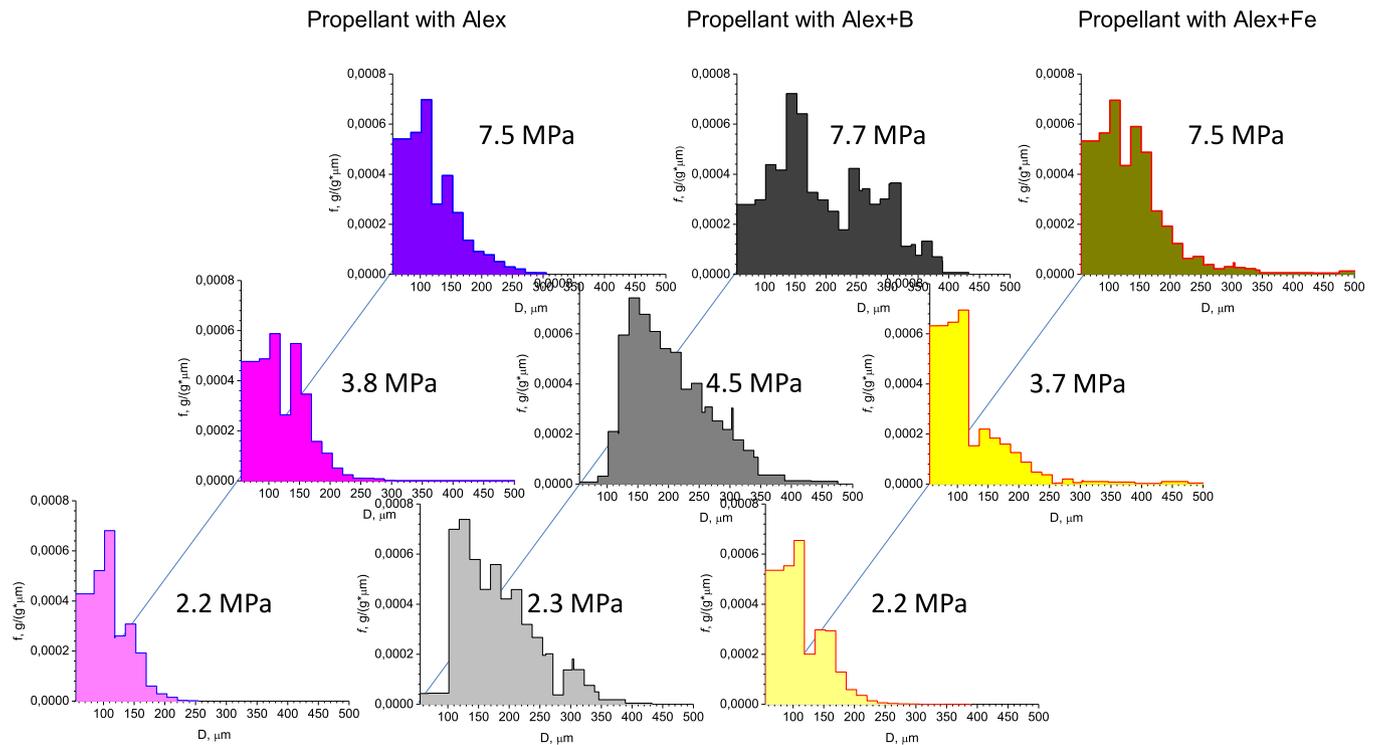

Fig. 5. Mass size distribution functions of agglomerate particles with size $D > D_L$ at different pressures.

diameter D_{43}^{ag} is changed as follows: $177\,\mu m \rightarrow 203\,\mu m \rightarrow 195\,\mu m$ ($\pm 9\,\mu m$).

In the case of propellant with Alex+Fe the form and parameters of particles size distribution are mainly similar to those for propellant with Alex (Fig. 5). The values of the combustion incompleteness η are close to each other, $0.030 \rightarrow 0.021 \rightarrow 0.029$ for Alex+Fe propellant and $0.033 \rightarrow 0.023 \rightarrow 0.020$ for Alex propellant (Table 2).

The observed transformation of functions of CCPs particle size distribution, caused by more efficient burning out of aluminum upon increasing the pressure, can be explained by the action of oppositely acted factors. It is known [44] that the small size particles burn out faster (in terms of metallic aluminum consumption rate) than the coarse ones. It is also known [45] that the fraction of aluminum oxide, which is accumulated on the surface of burning Al particles in the form of cap, is increased with the growth of

particle diameter. In accordance with the data of Table 2, the combustion incompleteness η of aluminum for propellant with Alex+B is approximately twice higher than that for propellants with Alex and Alex+Fe. Thus, the larger quantity of unburned metal is caused by the larger mass of agglomerates despite the metal content in the agglomerates of propellant with Alex+B is lower than that in the case of propellant with Alex. The tested propellants have the same geometric structure and comparable levels of the burning rate. Consequently, the thickness of the preheated and reaction layers of CSPs is also comparable. The propellant with Alex+B, compared with propellant with Alex, forms a larger mass of coarse agglomerate particles, which are characterized by a more complete combustion of metallic aluminum.

Plausible explanation is as follows. Owing to high melting point of boron (2573 K) the solid boron particles probably can be
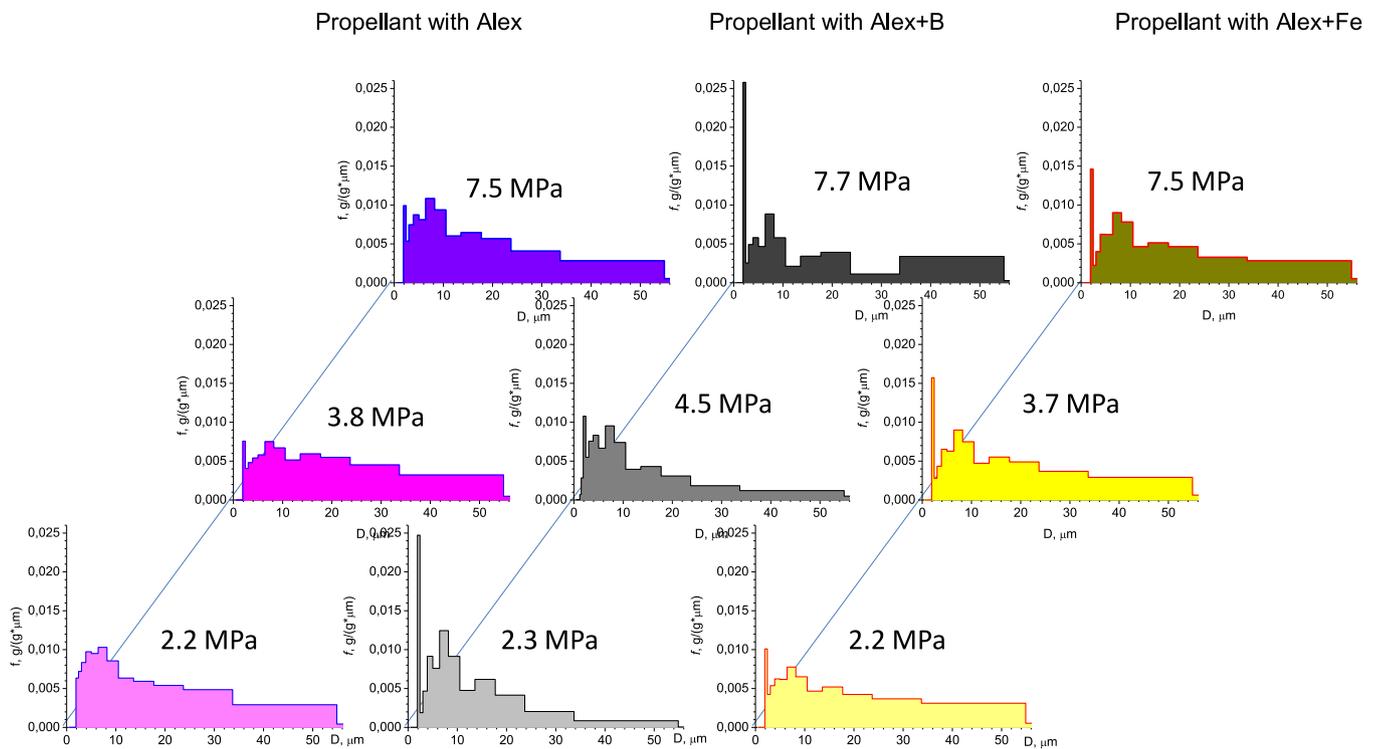
Propellant with Alex   Propellant with Alex+B   Propellant with Alex+Fe

Fig. 6. Mass size distribution functions of oxide particles with size $D < D_L$ at different pressures.

Table 3
Phase composition of oxide particles sampled in combustion of propellants.

Propellant No., metal fuel	p, MPa	Content of the crystal phase, wt.%					
		α-Al_2O_3	θ-Al_2O_3	γ-Al_2O_3	χ-Al_2O_3	C_3N_4	Others
1, Alex	2.2	2.7	35.4	–	17.6	44.3	–
	3.8	11.3	32.4	33.7	10.3	12.3	–
	7.5	8.4	42.8	–	12.2	36.6	–
2, Alex+Fe	2.2	5.4	23.0	–	28.6	40.3	2.7 Fe_3C
	3.7	5.4	54.8	16.4	–	23.4	–
	7.5	7.9	17.2	–	35.8	36.0	3.1 Fe_3C
3, Alex+B	2.3	5.8	30.7	–	17.8	22.5	23.2 $Al_4B_2O_9$
	4.5	35.3	13.3	5.0	–	6.7	39.7 $(Al_2O_3)_{10}(B_2O_3)_2$
	7.7	5.6	13.9	–	17.1	12.2	51.2 $Al_4B_2O_9$

captured by aluminum agglomerate in the course of its formation. Oxidation of high-disperse particles of aluminum and boron in the propellant in the process of the agglomerate formation begins at temperatures about of 723–973 K. It is expected that the inclusions of boron particles will lead to surface discontinuity of the aluminum oxide layer and to reducing its protective properties. As a result the aluminum ignition will become easier and transition from heterogeneous to vapor oxidation regime will happen earlier. The latter may result in decrease in the size of oxide particles. At the same time more pronounced aluminum oxidation in subsurface layer almost certainly promotes increase in the agglomerate size due to the mechanism described for the nitramine contained propellants. Namely, the results of [7,46] indicate that in the case of propellants containing RDX and HMX, whose decomposition temperature is significantly lower than that for AP, the cohesion strength holding the agglomerate on the surface is increased with the increase in completeness of metal oxidation in the subsurface layer. This is manifested in a positive correlation between the particles size and oxide content in the agglomerates. In other words, if the aluminum earlier gets oxidizing agents from the decomposition of the propellant components, then it is oxidized in a higher extent. The greater the fraction of oxide in the agglomerate, the stronger agglomerate is held on the burning surface and grows to a larger size.

Thus, the effect of boron additive is ambiguous. On the one hand, the supposed facilitation of ignition of aluminum provides more efficient combustion of aluminum and therefore percentage of the unburned aluminum in agglomerates of a propellant with Alex+B is actually lower than that for agglomerates of a propellant with Alex. On the other hand, assumed more effective holding of agglomerates on the burning surface may lead to increase in their sizes and masses that finally provide detected total incompleteness of aluminum in combustion products.

Additive of iron UFP does not make the pronounced effect on holding the agglomerates on the burning surface. According to the DTA data, the beginning temperature of intensive decomposition is decreased and the burning rate is increased. One can assume that in the case of propellant with Alex+Fe the increase in the cohesion strength as a result of the metal oxidation is compensated by increase in the detachment force due to increase value of outflow velocity of gasification products from the burning surface. In addition, a carbon-based skeleton-layer is formed on the burning surface of CSP sample, which facilitates the formation of agglomerate particles.

3.2.2. Oxide particles

As can be seen from Table 2, in all cases the aluminum content in the sieved fraction of <80 μm does not exceed 1.3 wt.%. It can be expected that the particles smaller than 55 μm have unburned aluminum content even less. Therefore, the fine particles of CCPs with $D < D_L$ can be considered as oxide particles. Examination of the mass size distribution of oxide particles smaller than 55 μm showed the following (Fig. 6).

In all cases (except for propellant with Alex at $p = 2.2$ MPa) the basic modes of size distributions are in the same ranges of particle size analyzer Malvern. Thus, the first mode is observed in the range of 1.9–2.4 μm, most «massive» mode is in the range of 3–11 μm. In the case of propellants with Alex+B and Alex+Fe amplitude of the first mode is much larger than in the case of propellant with Alex. The formation of micron and submicron sized particles is commonly associated with the vapor type combustion of aluminum [47]. Actually, the mass size distributions of fine particles for studied CSPs have different ratios of mode amplitudes and they are slightly changed with the pressure, Fig. 6. The variation of the ratio of modes results in different magnitudes of the mean diameters D_{30}^{ox}: for propellants with Alex, Alex+B and Alex+Fe they comprise about 6.4 μm, 4.8 μm and 5.9 μm, respectively (see Table 2).

3.2.3. Phase composition of oxide particles

X-ray analysis of sampled oxide particles of less than 80 μm fraction was performed via using the X-ray diffractometer Shimadzu XRD 6000. Typical X-ray diffraction patters are shown in Fig. 7. The data analysis showed that the content of amorphous phases in the sampled oxide particles of CCPs amounts to ~ 35 wt.% for propellant with Alex, to ~ 30 wt.% for propellant with Alex+Fe and to ~ 25 wt.% for propellant with Alex+B combusted at the pressure of 2.2 MPa. With the increase in pressure in the combustion chamber up to 7.5 MPa the content of amorphous phases in the composition of CCPs is decreased to ~ 20 wt.% for propellant with Alex and to ~ 15 wt.% for propellant with Alex+B. For propellant with Alex+Fe the content of amorphous phases in CCPs was practically unchanged and remained constant within the range of measurement error. The phase composition of crystalline oxide particles of CCPs for the tested CSPs excluding the amorphous phases is presented in Table 3.

Note the presence of crystalline phase of carbon nitride C_3N_4 for all tested CSPs (up to 44 wt.% in the case of propellant with Alex at $p = 2.2$ MPa). Partial replacement of Alex by boron in the composition of CSP leads to the reduction of carbon nitride C_3N_4 content by 2–3 times in CCPs.

Analysis of the mass and size parameters of CCPs in the examined pressure range of 2.2–7.5 MPa (Table 3) showed the following. Replacement of 2 wt.% Alex by boron in the CSP leads to significant increase in the agglomerates fraction m_{ag}/m_{ccp} in sampled CCPs (by 1.8–2.2 times) and 1.6–1.7 fold increase in the mean diameter D_{43}^{ag}. At the same time the fraction of oxide particles in CCPs m_f/m_{ccp} is reduced by 1.2–1.3 times and the mean diameter D_{30}^{ox} by 1.3–1.4 times.

Thus, partial replacement of 2 wt.% Alex by iron in the CSP formulation leads to the increase in agglomerate particle content m_{ag}/m_{ccp} in CCPs by 1.1–1.4 times and in the mean diameter of agglomerates D_{43}^{ag} by 1.03–1.18 times. At the same time the content of oxide particles m_f/m_{ccp} in the composition of CCPs and the mean diameter D_{30}^{ox} are decreased by 1.01–1.05 times and by 1.05–1.16 times, respectively.

4. Conclusions

1. Effect of ultrafine iron and amorphous boron additives in CSP formulations based on AP, butadiene rubber and Alex on the
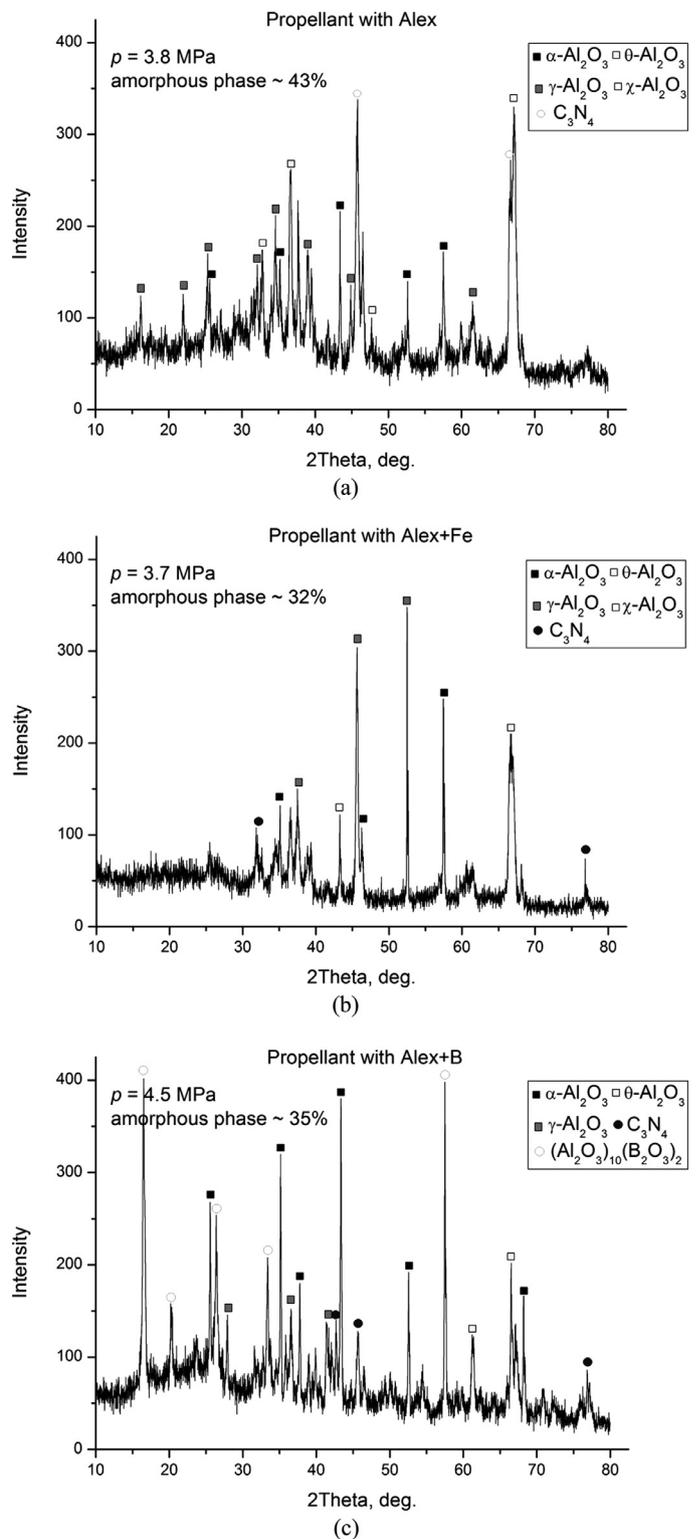

Fig. 7. X-ray diffraction patterns of oxide particles sampled in combustion process of propellants with Alex (a), Alex+Fe (b) and Alex+B (c) at pressure ~ 4 MPa.

combustion characteristics was studied. Dependency of the burning rate on pressure and particle size distribution and phase composition of sampled condensed combustion products were determined.

2. It was found that partial Alex replacement (2% within 15.7%) by iron UFP in the formulation of CSP leads to 1.3–1.4 fold increase in the burning rate in the pressure range of 2.2–7.5 MPa. At the

same time the agglomeration extent of metal fuel is slightly increased: the mean diameter of agglomerate particles is increased by 1.2 fold and the content of agglomerates in the CCPs composition is increased by 1.4 fold. The content and mean diameter D_{30} of oxide particles in CCPs are reduced by 16% and 13%, respectively.

3. Upon partial Alex replacement (2% within 15.7%) by boron UFP the burning rate is practically unchanged with respect to the basic propellant with Alex in the pressure range of 2.2–7.5 MPa. However, the agglomeration extent is significantly enhanced, which is manifested by the increase in the agglomerates content in CCPs composition by 1.8–2.2 times and by 1.6–1.7 times increase in the agglomerates mean diameter. It is manifested as well as by increase in the metal fraction, which is involved in agglomerates formation, by 1.6–1.9 times. The content and the mean diameter D_{30}^{ox} of the oxide particles in CCPs are reduced more significantly than those upon introduction of iron by 1.2–1.3 times and 1.3–1.4 times, respectively.

4. Practical application can find the following findings. (1) The increase in the burning rate of CSPs based on AP, butadiene rubber and Alex, by 30–40% without changing the value of the pressure exponent via introducing the iron additive. (2) The reduction of the mean diameter D_{30}^{ox} of oxide particles of CCPs by 30–40% via introducing the boron additive.

However, it should be kept in mind that introducing both additives leads to enhancement of agglomeration extent, which is especially significant in the case of boron. This also leads to the reduction of theoretical specific impulse by 3% in the case of iron additive. Experimentally shown that in the case of boron additive the combustion products contain significant amount of crystalline carbon nitride C_3N_4. This material becomes at present called-for due to a number of exceptional properties [48,49].

Acknowledgment

References

[1] M.W. Beckstead, K. Puduppakkama, P. Thakreb, V. Yang, Modeling of combustion and ignition of solid-propellant ingredients, Prog. Energy Combust. Sci. 33 (2007) 497–551.

[2] M. Kohga, K. Okamoto, Thermal decomposition behaviors and burning characteristics of ammonium nitrate/polytetrahydrofuran/glycerin composite propellant, Combust. Flame 158 (2011) 573–582.

[3] V.A. Arkhipov, A.G. Korotkikh, The influence of aluminum powder dispersity on composite solid propellants ignitability by laser radiation, Combust. Flame 159 (2012) 409–415.

[4] L. DeLuca, F. Cozzi, G. Germiniasi, I. Ley, A.A. Zenin, Combustion mechanism of an RDX-based composite propellant, Combust. Flame 118 (1999) 248–261.

[5] K. Takahashi, S. Oide, T. Kuwahara, Agglomeration characteristics of aluminum particles in AP/AN composite propellants, Propellants, Explosives, Pyrotech. 38 (2013) 555–562.

[6] N. Muravyev, Y. Frolov, A. Pivkina, K. Monogarov, O. Ordzhonikidze, I. Bushmarinov, A. Korlyukov, Influence of particle size and mixing technology on combustion of HMX/Al compositions, Propellants, Explosives, Pyrotechnics 35 (2010) 226–232.

[7] O.G. Glotov, Condensed combustion products of aluminized propellants. IV. Effect of the nature of nitramines on aluminum agglomeration and combustion efficiency, Combust., Explos. Shock Waves 42 (2006) 436–449.

[8] T.D. Hedman, L.J. Groven, R.P. Lucht, S.F. Son, The effect of polymeric binder on composite propellant flame structure investigated with 5 kHz OH PLIF, Combust. Flame 160 (2013) 1531–1540.

[9] V.A. Arkhipov, S.S. Bondarchuk, A.G. Korotkikh, V.T. Kuznetsov, A.A. Gromov, S.A. Volkov, L.N. Revyagin, Influence of aluminum particle size on ignition and nonstationary combustion of heterogeneous condensed systems, Combust. Explos. Shock Waves 48 (2012) 625–635.

[10] V.A. Arkhipov, A.G. Korotkikh, V.T. Kuznetsov, A.A. Razdobreev, I.A. Evseenko, Influence of the dispersity of aluminum powder on the ignition characteristics of composite formulations by laser radiation, Russ. J. Phys. Chem. B 5 (2011) 616–624.

[11] M.V. Komarova, V.F. Komarov, A.G. Vakutin, A.V. Yaschenko, Effect of nanosize bimetallic particles on the combustion characteristics of composite propellant, Polzunovsky Vestnik 4 (2010) 112–116.

[12] T.D. Hedman, D.A. Reese, K.Y. Cho, L.J. Groven, R.P. Lucht, S.F. Son, An experimental study of the effects of catalysts on an ammonium perchlorate based composite propellant using 5 kHz PLIF, Combust. Flame 159 (2012) 1748–1758.

[13] V.A. Arkhipov, S.S. Bondarchuk, A.G. Korotkikh, Comparative analysis of methods for measuring the transient burning rate. II. Research results, Combust. Explos. Shock Waves 46 (2010) 570–577.

[14] S. Shioya, M. Kohga, T. Naya, Burning characteristics of ammonium perchlorate-based composite propellant supplemented with diatomaceous earth, Combust. Flame 161 (2014) 620–630.

[15] K. Ishitha, P.A. Ramakrishna, Studies on the role of iron oxide and copper chromite in solid propellant combustion, Combust. Flame 161 (2014) 2717–2728.

[16] C.W. Farley, M.L. Pantoya, V.I. Levitas, A mechanistic perspective of atmospheric oxygen sensitivity on composite energetic material reactions, Combust. Flame 161 (2014) 1131–1134.

[17] V.A. Arkhipov, A.G. Korotkikh, A.A. Gromov, V.T. Kuznetsov, A.V. Pesterev, I.A. Evseenko, Effect of catalytic additives of metal powders on the high energy materials ignition, Russ. Phys. J. 54 (2011) 299–306.

[18] B.A. McDonald, J.R. Rice, M.W. Kirkham, Humidity induced burning rate degradation of an iron oxide catalyzed ammonium perchlorate/HTPB composite propellant, Combust. Flame 161 (2014) 363–369.

[19] M.K. Berner, M.B. Talawar, V.E. Zarko, Nanoparticles of energetic materials: synthesis and properties (Review), Combust. Explos. Shock Waves 49 (2013) 625–647.

[20] V.A. Arkhipov, A.B. Kiskin, V.E. Zarko, A.G. Korotkikh, Laboratory method for measurement of the specific impulse of solid propellants, Combust. Explos. Shock Waves 50 (2014) 622–624.

[21] G.V. Sakovich, V.A. Arkhipov, A.B. Vorozhtsov, A.G. Korotkikh, Solid rocket propellants based on the dual oxidizer containing the aluminum ultra-fine powder, Bull. Tomsk Polytech. Univ. 314 (2009) 18–22.

[22] V.F. Komarov, M.V. Komarova, A.B. Vorozhtsov, M.I. Lerner, V.V. Domashenko, Processes proceeding in high-energy systems comprising nanodimensional aluminum and other nanometals, Russ. Phys. J. 56 (2013) 365–369.

[23] V.A. Arkhipov, T.I. Gorbenko, M.V. Gorbenko, A.V. Pesterev, L.A. Savel'eva, Effect of catalytic additives and aluminum particle size on the combustion of mixed compositions with a chlorine-free oxidizer, Combust. Explos. Shock Waves 48 (2012) 642–649.

[24] T.R. Sippel, S.F. Son, L.J. Groven, Aluminum agglomeration reduction in a composite propellant using tailored Al/PTFE particles, Combust. Flame 161 (2014) 311–321.

[25] A. Sossi, E. Duranti, M. Manzoni, C. Paravan, L.T. DeLuca, A.B. Vorozhtsov, M.I. Lerner, N.G. Rodkevich, A.A. Gromov, E.N. Savin, Combustion of HTP-B-based solid fuels loaded with coated nanoaluminum, Combust. Sci. Technol. 185 (2013) 17–36.

[26] Y. Aly, M. Schoenitz, E.L. Dreizin, Ignition and combustion of mechanically alloyed Al-Mg powders with customized particle sizes, Combust. Flame 160 (2013) 835–842.

[27] Y.L. Shohin, R.S. Mudryy, E.L. Dreizin, Preparation and characterization of energetic Al-Mg mechanical alloy powders, Combust. Flame 128 (2002) 259–269.

[28] K. Hori, O.G. Glotov, V.E. Zarko, H. Habu, A.M.M. Faisal, T.D. Fedotova, Study of the combustion residues for Mg/Al solid propellant, Energetic Materials – Synthesis, Production and Application: 33rd International Annual Conference of Fraunhofer ICT (2002), pp. 71-1–71-14.

[29] O.G. Glotov, V.N. Simonenko, V.E. Zarko, R.K. Tukhtaev, T.F. Grigoryeva, T.D. Fedotova, Combustion characteristics of propellants containing aluminum-boron mechanical alloy, Energetic Materials – Structure and Properties, 35th International Annual Conference of Fraunhofer ICT (2004), pp. 107-1–107-18.

[30] O.G. Glotov, V.E. Zarko, V.N. Simonenko, T.D. Fedotova, R.K. Tukhtaev, T.F. Grigoryeva, Effect of Al/B mechanical alloy on combustion characteristics of AP/HMX/energetic binder propellants, Energetic Materials – Performance and Safety: 36th International Annual Conference of Fraunhofer ICT & 32nd International Pyrotechnics Society (2005) 102-1–102-12.

[31] O.G. Glotov, D.A. Yagodnikov, V.S. Vorob'ev, V.E. Zarko, V.N. Simonenko, Ignition, combustion, and agglomeration of encapsulated aluminum particles in a composite solid propellant. II. Experimental studies of agglomeration, Combust. Explos. Shock Waves 43 (2007) 320–333.

[32] Y.F. Ivanov, M.N. Osmonoliev, V.S. Sedoi, V.A. Arkhipov, S.S. Bondarchuk, A.B. Vorozhtsov, A.G. Korotkikh, V.T. Kuznetsov, Productions of ultra-fine powders and their use in high energetic compositions, Propellants Explosives Pyrotech. 28 (2003) 319–333.

[33] A. Gromov, U. Teipel, Metal nanopowders: production, characterization, and energetic applications, Wiley Blackwell, 2014, p. 417.

[34] O.G. Glotov, V.Ya. Zyryanov, Condensed combustion products of aluminized propellants. I. A technique for investigating the evolution of disperse-phase particles, Combust. Explos. Shock Waves 31 (1995) 72–78.

[35] T.D. Fedotova, O.G. Glotov, V.E. Zarko, Chemical analysis of aluminum as a propellant ingredient and determination of aluminum and aluminum nitride in condensed combustion products, Propellants Explos. Pyrotech. 25 (2000) 325–332.

[36] V.E. Zarko, O.G. Glotov, Formation of Al oxide particles in combustion of aluminized condensed systems (Review), Sci. Technol. Energ. Mater. 74 (2013) 139–143.

[37] V.A. Babuk, V.A. Vasilyev, M.S. Malachov, Condensed combustion products at the burning surface of aluminized solid propellant, J. Propuls. Power 15 (1999) 783–793.

[38] T.D. Fedotova, O.G. Glotov, V.E. Zarko, Application of cerimetric methods for determining the metallic aluminum content in ultrafine aluminum powders, Propellants Explos. Pyrotech. 32 (2007) 160–164.

[39] B.G. Trusov, Code system for simulation of phase and chemical equilibriums at higher temperatures, Eng. J.: Sci. Innov. 1 (2012) 21–30.

[40] A.G. Korotkikh, V.A. Arkhipov, O.G. Glotov, A.B. Kiskin, V.E. Zarko, Effect of iron powder on ignition and combustion characteristics of composite solid propellants, Khimicheskaya Fizika I Mezoskopiya 1 (2015) 12–22.

[41] A.G. Korotkikh, V.A. Arkhipov, O.G. Glotov, A.B. Kiskin, Effect of metal additives on the thermal decomposition and ignition of composite solid propellants with Alex, Energetic Materials – Synthesis, Characterization, Processing: 47th International Annual Conference of Fraunhofer ICT (2016), pp. 133-1–133-9.

[42] A.G. Korotkikh, V.A. Arkhipov, A.A. Ditts, S.A. Yankovskiy, Influence of powder additives of titanium, boron ad iron on the energy characteristics of heterogeneous condensed systems, Russ. Phys. J. 9-3 (2014) 108–113.

[43] O.G. Glotov, A.G. Korotkikh, V.A. Arkhipov, A.B. Kiskin, V.E. Zarko, O.N. Zhitnitsky, G.S. Surodin, Condensed combustion products of solid propellant with boron additive, Energetic Materials – Performance, Safety and System Applications: 46th International Annual Conference of Fraunhofer ICT (2015), pp. 123-1–123-12.

[44] O.G. Glotov, V.E. Zarko, V.V. Karasev, T.D. Fedotova, A.D. Rychkov, Macrokinetics of combustion of monodisperse agglomerates in the flame of a model solid propellant, Combust. Explos. Shock Waves 39 (2003) 552–562.

[45] O.G. Glotov, V.A. Zhukov, The evolution of 100-µm aluminum agglomerates and initially continuous aluminum particles in the flame of a model solid propellant. II. Results, Combust., Explos. Shock Waves 44 (2008) 671–680.

[46] S. Suzuki, Combustion Efficiency of Aluminized Propellants (1989) 1–8 AIAA Meeting Papers, 89-2309.

[47] O.G. Glotov, Condensed combustion products of aluminized propellants. III. Effect of an inert gaseous combustion environment, Combust. Explos. Shock Waves 38 (2002) 92–100.

[48] D.R. Miller, J. Wang, E.G. Gillan, Rapid, facile synthesis of nitrogen-rich carbon nitride powders, J. Mater. Chem. 12 (2002) 2463–2469.

[49] A. Thomas, A. Fischer, F. Goettmann, M. Antonietti, J.-O. Muller, R. Schlogl, J.M. Carlsson, Graphitic carbon nitride materials: variation of structure and morphology and their use as metal-free catalysts, J. Mater. Chem. 18 (2008) 4893–4908.